Fluorescence lifetime detection in turbid media using spatial frequency domain filtering of time domain measurements

Anand T. N. Kumar

Athinoula A. Martinos Center for Biomedical Imaging, Department of Radiology, Massachusetts General Hospital, Harvard Medical School, Charlestown, Massachusetts 02129, USA (ankumar@nmr.mgh.harvard.edu)

Received February 20, 2013; accepted March 22, 2013;
posted March 25, 2013 (Doc. ID 185682); published April 24, 2013

It is demonstrated that high spatial frequency filtering of time domain fluorescence signals can allow efficient detection of intrinsic fluorescence lifetimes from turbid media and the rejection of diffuse excitation leakage. The basis of this approach is the separation of diffuse fluorescence signals into diffuse and fluorescent components with distinct spatiotemporal behavior. © 2013 Optical Society of America

OCIS codes: (170.3880) Medical and biological imaging; (170.6920) Time-resolved imaging; (170.6960) Tomography.
http://dx.doi.org/10.1364/OL.38.001440

The temporal decay time constant (lifetime) of fluorescence from a turbid medium, such as tissue can, in general, depend on the intrinsic absorption and scattering coefficients [1]. Unless the fluorescence lifetime is significantly longer than the intrinsic diffusion timescales ($\sim 10^{-9}$ s) [2], a robust recovery of the intrinsic lifetimes necessitates the inversion of coupled differential equations for fluorescence propagation in tissue [3], which can be ill-posed. In this Letter, it is shown that direct recovery of shorter *in vivo* lifetimes is possible with time domain (TD) measurements, by exploiting a unique phenomenon, namely the separation of diffuse fluorescence into diffuse and pure fluorescent decay terms that exhibits distinct spatiotemporal responses. In the spatial frequency domain (FD), the diffuse term decays at a rate proportional to the spatial frequency, tissue absorption, and scattering (analogous to the temporal propagation of intrinsic diffuse light [4,5]). However, the decay of the fluorescence term is independent of spatial frequency or optical properties but reflects the characteristic lifetime of the fluorophore in the tissue environment. The fluorescence therefore remains significant at high spatial frequencies, where the diffuse term is rapidly eliminated. This observation has important implications for macroscopic lifetime imaging in turbid media. In particular, we show experimentally that it allows direct detection of lifetimes shorter than the intrinsic diffuse timescales, and discrimination of fluorescence from diffuse excitation leakage through emission filters, a common problem encountered in fluorescence imaging.

Consider a diffuse medium with optical properties $(\mu_a^x(\mathbf{r}),\ \mu_s^x(\mathbf{r}))$ at the excitation and $(\mu_a^m(\mathbf{r}),\ \mu_s^m(\mathbf{r}))$ at the emission wavelengths, with fluorophores described by yield distributions $\eta_n(\mathbf{r})$ and lifetimes $\tau_n = 1/\Gamma_n$. Using complex integration methods, it can be shown [1] that the TD fluorescence intensity at position $\mathbf{r}_d$ and time t for point excitation at $\mathbf{r}_s$ can be written as $U_F = \sum_n U_{Fn}$, where (for the case $\Gamma_n < v\mu_a^{x,m}$)

$$U_{Fn}(\mathbf{r}_s, \mathbf{r}_d, t) = -a_{Dn}(\mathbf{r}_s, \mathbf{r}_d, t) + a_{Fn}(\mathbf{r}_s, \mathbf{r}_d)e^{-\Gamma_n t}. \quad (1)$$

Here $a_{Fn} = \int_\Omega \mathrm{d}^3 r \tilde{W}(\mathbf{r}_s, \mathbf{r}_d, \mathbf{r}, -i\Gamma)\eta_n(\mathbf{r})$ is the fluorescence decay amplitude of the nth lifetime species, valid for arbitrary heterogeneous transport media [6], where Ω is the medium volume and $\tilde{W} = \tilde{G}^x(\mathbf{r}_s, \mathbf{r}, \omega)\tilde{G}^m(\mathbf{r}_d, \mathbf{r}, \omega)$ is the FD weight function with $\tilde{G}^{x,m}$ as the Green's functions of the FD diffusion equation. For a homogeneous medium with $\mu_a^x = \mu_a^m = \mu_a$,

$$a_{Dn} = \int_\Omega \mathrm{d}^3 r \left[\frac{1}{\pi}\int_{v\mu_a}^\infty \mathrm{d}\gamma \frac{\mathrm{Im}[\tilde{W}(\mathbf{r}_s, \mathbf{r}_d, \mathbf{r}, -i\gamma)]}{\gamma - \Gamma_n} e^{-\gamma t}\right]\eta_n(\mathbf{r}) \quad (2)$$

is the diffusive term arising from the branch points of the FD weight function [1], where Im refers to the imaginary part. Note that a_{Dn} involves $\tilde{W}$ at an imaginary frequency of $-i\gamma$, which is equivalent to a CW weight function with a negative absorption of $\mu_a(\mathbf{r}) - \gamma/v$, while a_{Fn} involves $\tilde{W}$ at a reduced absorption of $\mu_a - \Gamma_n/v$.

The central point of this Letter is that a_{Fn} is independent of time, whereas a_{Dn} propagates similarly to intrinsic diffuse light through tissue [5]. To see this, consider the spatial Fourier transform of U_F w.r.t $\mathbf{r}_d$:

$$\tilde{U}_{Fn}(\mathbf{r}_s, \mathbf{k}_d, t) = -\tilde{a}_{Dn}(\mathbf{r}_s, \mathbf{k}_d, t) + \tilde{a}_{Fn}(\mathbf{r}_s, \mathbf{k}_d)e^{-\Gamma_n t}. \quad (3)$$

The distinct spatiotemporal behavior of a_D and a_F and the k-space transforms, $\tilde{a}_D$, and $\tilde{a}_F$, is illustrated in Fig. 1 using simulations with a diffusive slab model ($\mu_a = 0.2$/cm, $\mu_s' = 10$/cm) with a fluorescent inclusion ($\tau = 0.3$ ns). The spatial profile of $U_F(\mathbf{r}_s, \mathbf{r}_d, t)$ expands with time, approaching a_F asymptotically [Fig. 1(b)]. Figure 1(c) shows the separation of U_F into a diffusive contribution, a_D, with a spatial distribution that expands over time, and a time-independent contribution from a_F. Correspondingly, Fig. 1(d) shows $\tilde{U}_F$ decomposed into a spatially narrowing $\tilde{a}_D$ and a stationary $\tilde{a}_F$.

The rapid decrease of high spatial frequencies of $\tilde{a}_D$ is similar to that of intrinsic diffuse signals [5], and suggests that both of these contributions can be minimized in fluorescence signals by spatial filtering, as we demonstrate using a simple phantom experiment. A small tube was placed near the bottom of a 1.75 cm thick intralipid phantom ($\mu_s' \approx 22$/cm, $\mu_a \approx 0.02$/cm). The tube was filled with 100 μL of 1 μM IRdye800 (LI-COR Biosciences) in either water [$\tau = 0.4$ ns, Fig. 2(b)] or glycerol solvents

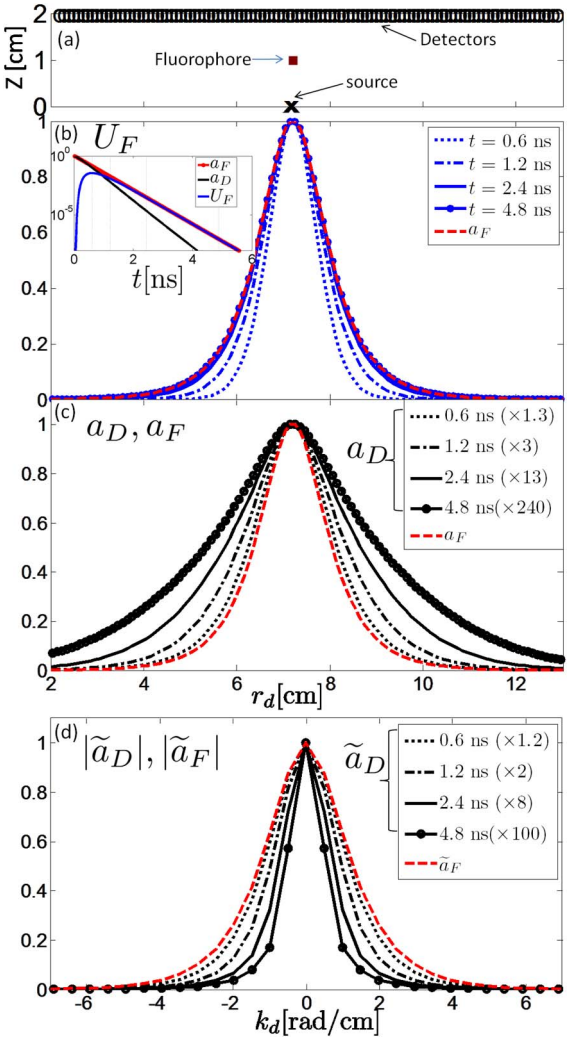

Fig. 1. (a) Simulation geometry indicating the source (x) and detectors (o) with a single fluorophore ($\tau = 0.3$ ns) at the center. (b) Normalized TD fluorescence signal U_F as a function of $\mathbf{r}_d$ at various times. Inset shows U_F (blue) at the central detector as a function of t, separated into a_D (black) and a_F (red). (c) Separation of U_F into a spatially spreading diffuse amplitude a_D (black) and a stationary fluorescent amplitude a_F (red). (d) Separation of $\tilde{U}_F$ into a spatially narrowing $\tilde{a}_D$ and stationary $\tilde{a}_F$. (All curves normalized to the maximum of a_F at each time point with scaling factors indicated.)

[$\tau = 0.72$ ns, Fig. 2(c)], and excited in the transmission geometry with a Ti:sapphire laser at 790 nm. Detection was performed with a $\lambda > 800$ nm emission filter attached to an intensified CCD camera (PicostarHR, LAVision, Gmbh; 300 ps gatewidth, 560 V gain, 100 ps steps, 4×4 software binning). The excitation wavelength was chosen close to the filter passband to allow leakage of the diffuse excitation light into the filter, to demonstrate its subsequent elimination by spatial Fourier filtering. The full TD data was collected for two source positions 1 cm apart below the phantom, one directly below the fluorescent tube [S_2, Figs. 2(b) and 2(c)], and the other 1 cm away from the tube [S_1, Fig. 2(a)]. The CW (integrated TD) images [Figs. 2(d)–2(f)] do not distinguish either source positions or lifetimes in the tube within the phantom. Moreoever, the lifetime maps obtained from single-exponential fits to the asymptotic TD decay

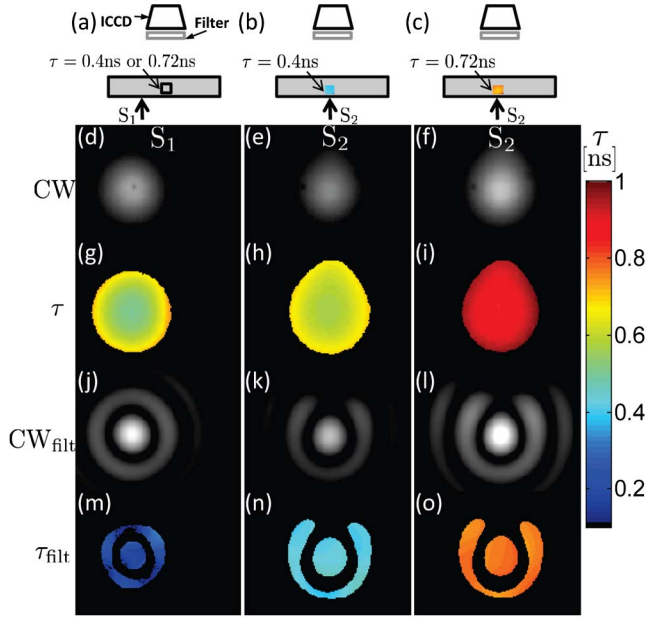

Fig. 2. Measurement setup up with a 1.75 cm thick intralipid phantom excited at 790 nm at (a) S_1 and (b),(c) S_2, and detected with a $\lambda > 800$ nm filter. The tube with IRdye800 is shown schematically (color depicts true lifetime) in (b) with water (0.4 ± 0.01 ns) and (c) with 50% glycerol (0.72 ± 0.02 ns). The CW diffuse fluorescence images and lifetime maps are shown in (d) and (g) for source S_1 (similar for both lifetimes), (e) and (h) for S_2 with 0.4 ns dye, (f) and (i) for S_2 with 0.7 ns dye. (j)–(l) k-space filtered CW intensity $\int dt U^{\text{filt}}$ [Eq. (4)]. (m)–(o) Lifetime maps (τ_{filt}) from fits to decay of $U^{\text{filt}}(t)$.

[Figs. 2(g)–2(i)] do not reflect the true lifetimes of the fluorophores due to the influence of tissue propagation on the TD decays and excitation. Note the increase in lifetime from the center of the image toward the edge, due to a larger propagation distance from the source. The signal for S_1 was negligible for 770 nm excitation (not shown), while the lifetime map at 790 nm [Fig. 2(g)] was similar to that without any emission filter (not shown), confirming that the signal for the S_1 case is diffuse excitation leakage, which, in the present case, is indistinguishable from the 0.4 ns dye [Fig. 2(h)].

A spatial 2D fast Fourier transform (FFT) in MATLAB (The Mathworks Inc.,) was applied to the 2D spatial TD data thresholded at 3% of the maximum intensity, resulting in the full detector spatial frequency (k-space) TD data for all delays. The k-space lifetime maps (Fig. 3) obtained from single-exponential fits to the decay portion of the k-space TD data show distinct behavior of the diffuse excitation [Fig. 3(a)] and fluorescence signals [Figs. 3(b) and 3(c)]; while the k-space lifetime for source S_1 (diffuse excitation/leakage) continuously decreases toward higher k's, the lifetime for fluorescence approaches the true fluorophore lifetimes of 0.4 ± 0.01 ns and 0.72 ± 0.02 ns. It is plausible to apply a high-frequency filter in k space to extract the intrinsic fluorescence. The choice of the appropriate filter will depend on rate of decay of the intrinsic lifetime maps (which depends on the tissue optical properties [7]). Here we choose an annular ring [Fig. 3(d)] of the form $f(\mathbf{k}_d) = \exp[-(k_x \cos(\theta) + k_y \sin(\theta) - R)^2/\sigma^2]$, where $R = |\mathbf{k}_d| =$

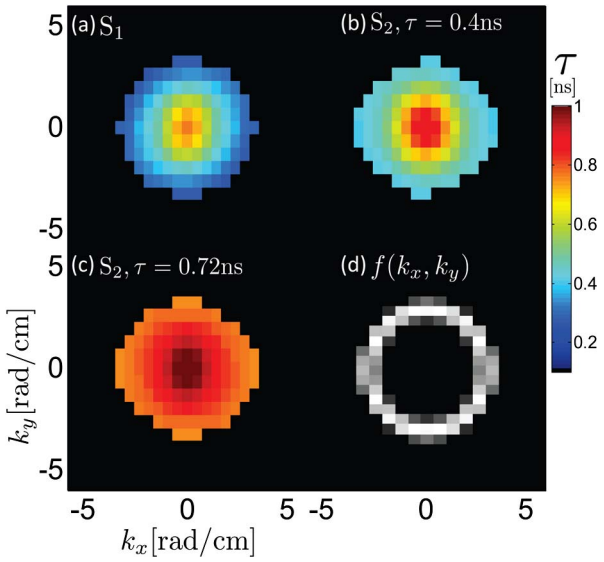

Fig. 3. Lifetime maps in spatial Fourier domain correponding to the TD data in Fig. 2 for (a) the diffuse signal/excitation leakage [S_1 in Fig. 2(a)], (b) 0.4 ns dye in intralipid, and (c) 0.72 ns dye in intralipid. (d) Spatial frequency filter.

$\sqrt{k_x^2 + k_y^2}$ and $\theta = \tan^{-1}[k_y/k_x]$ with $R = 3$ rad/cm and $\sigma = 1$ rad/cm. This eliminates the diffuse contribution from the low frequencies while also avoiding noisy data at high spatial frequencies. Subsequently, the spatial TD data is obtained as an inverse FFT:

$$U_F^{\text{filt}}(\mathbf{r}_s, \mathbf{r}_d, t) = \int \frac{\mathrm{d}^2 k_d}{(2\pi)^2} f(\mathbf{k}_d) \tilde{U}_F(\mathbf{r}_s, \mathbf{k}_d, t) e^{i\mathbf{k}_d \cdot \mathbf{r}_d}. \quad (4)$$

Single-exponential fits to the asymptotic decays of U_F^{filt} [Figs. 2(m)–2(o)] recover the true lifetimes [Figs. 2(b) and 2(c)] to within 5% and clearly distinguish the true fluorescence from diffuse excitation leakage [Fig. 2(m)], while the CW components, viz., $\int \mathrm{d}t U^{\text{filt}}(t)$ [Figs. 2(j)–2(l)] do not distinguish the three cases. Figure 4 shows a sample of raw TD data for a detector above the source and the spatial Fourier components for the 0.4 ns case. While the raw TD signals are similar for excitation leakage (black) and fluorescence (blue), the true lifetime of 0.4 ± 0.01 ns is recovered for source S_2 at $(k_x, k_y) = (4, 3)$ rad/cm, whereas the corresponding diffuse excitation leakage for S_1 decays at a much shorter rate (0.2 ns). Note the longer lifetime of $\tilde{U}_F(0, 0)$ for S_2, reflecting the longer lifetimes near the edge of the spatial lifetime map in Fig. 2(h).

In summary, an approach to extract fluorescence lifetimes from diffuse media was presented, based on spatial Fourier filtering of time-resolved data. The key principle is that the diffuse component of fluorescence signals decays at a rate that increases with spatial frequency, while the pure fluorescence component always decays at the intrinsic lifetime. This observation offers a

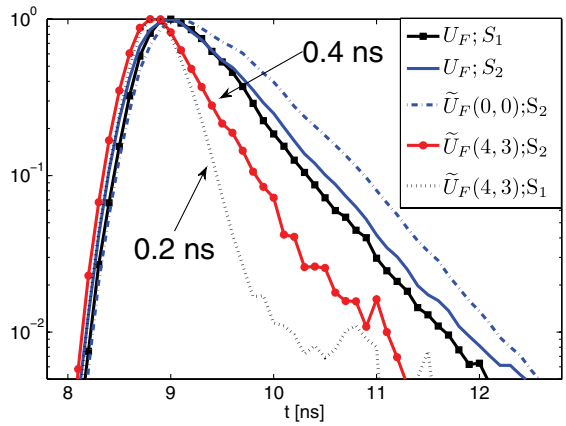

Fig. 4. Normalized raw TD data for a detector (3×3 pixel area) above the source with a 0.4 ns dye in intralipid [see Fig. 2(b)] for source S_1 (black line, square) and S_2 (blue line). The spatial Fourier components at $(k_x, k_y) = (4, 3)$ rad/cm are shown for S_2 (red line, filled circle) and S_1 (black dotted line) and at $(k_x, k_y) = (0, 0)$ for S_2 (blue dashed–dotted line).

powerful way to detect the presence of scattering or excitation leakage in biological lifetime measurements [8]. While only a single lifetime was considered in the experiments, the formalism presented here, is readily applicable to multiple lifetimes, and can also be extended to tomographic lifetime multiplexing [2] in the spatial Fourier domain. A novel aspect of this work is that the entire spectrum of detector side k-space amplitudes is obtained from the raw TD data with a simple FFT, without the need for complicated modulation techniques [5,9]. However, the extension of this approach to modulated excitation [5,7,9] can offer a powerful new approach for high-throughput tomographic lifetime imaging and will be considered in future work.

The author thanks Simon Arridge for useful discussions. This work was supported by the National Institutes of Health, grant R01 EB015325.

References

1. A. T. N. Kumar, J. Skoch, B. J. Bacskai, D. A. Boas, and A. K. Dunn, Opt. Lett. **30**, 3347 (2005).
2. S. B. Raymond, D. A. Boas, B. J. Bacskai, and A. T. N. Kumar, J. Biomed. Opt. **15**, 046011 (2010).
3. S. R. Arridge and J. C. Schotland, Inverse Probl. **25**, 123010 (2009).
4. M. S. Patterson, B. Chance, and B. C. Wilson, Appl. Opt. **28**, 2331 (1989).
5. A. Bassi, C. D'Andrea, G. Valentini, R. Cubeddu, and S. R. Arridge, Opt. Lett. **33**, 2836 (2008).
6. A. T. N. Kumar, S. B. Raymond, G. Boverman, D. A. Boas, and B. J. Bacskai, Opt. Express **14**, 12255 (2006).
7. D. J. Cuccia, F. Bevilacqua, A. J. Durkin, F. R. Ayers, and B. J. Tromberg, J. Biomed. Opt. **14**, 024012 (2009).
8. M. Y. Berezin and S. Achilefu, Chem. Rev. **110**, 2641 (2010).
9. J. Chen, V. Venugopal, F. Lesage, and X. Intes, Opt. Lett. **35**, 2121 (2010).